Distorted five-coordinate square pyramidal geometry of a cadmium(II) complex containing a 2-methylimidazole ligand: Crystal structure and axial ligand effect on spectroscopic properties

Chadlia Mchiri, Habib Nasri, Céline Frochot, Samir Acherar

Distorted five-coordinate square pyramidal geometry of a cadmium(II) complex containing a 2-methylimidazole ligand: Crystal structure and axial ligand effect on spectroscopic properties

Chadlia Mchiri,[a,b,✉] Habib Nasri,[b,✉] Céline Frochot,[c,✉] and Samir Acherar*[,a,✉]

[a] *Laboratoire de Chimie Physique Macromoléculaire (LCPM), Université de Lorraine, CNRS, 1 rue Grandville BP 20451, 54001 Nancy Cedex, France.*

[b] *Laboratoire de Physico-Chimie des Matériaux (LPCM), Faculté des Sciences de Monastir, Avenue de l'environnement, 5019 Monastir, University of Monastir, Tunisia.*

[c] *Laboratoire Réactions et Génie des Procédés (LRGP), Université de Lorraine, CNRS, 1 rue Grandville BP 20451, 54001 Nancy Cedex, France.*

Abstract

In this work, we describe a novel cadmium(II) complex based on the insertion of the Cd(II) metal ion into the *meso*-tetrakis(4-tert-butylphenyl)porphyrin (TBPP) ring, followed by the coordination of the 2-methylimidazole (2-MeHIm) *N*-donor axial ligand. Single crystal X-ray diffraction of [Cd(TBPP)(2-MeHIm)] (**I**) revealed that the Cd(II) metal ion induces a significantly distorted five-coordinate square pyramidal geometry of the metalloporphyrin (MP). This particular geometry provides a high displacement of the Cd(II) metal atom out of the porphyrinato mean plane by 0.860 Å, which is slightly higher than in related [Cd(II)(porphyrin)(ligand)] complexes. This high value induces a significant porphyrinato core *doming* and a moderate *ruffling*. An UV-visible spectroscopy study highlighted the red-shift effect of the absorption bands after the insertion of the Cd(II) metal ion into the TBPP ring and this effect is greater after coordination of the 2-MeHIm axial ligand. The calculated Gap energy E_g from the UV-visible spectra indicate interesting organic semiconducting properties. A fluorescence emission spectroscopy study showed a remarkable blue-shift effect in the Q bands accompanied by a decrease of the fluorescence emission, quantum yield (ϕ_f) and lifetime (τ_f) after the insertion of Cd(II) metal ion into TBPP, while the coordination of 2-MeHIm axial ligand had a minor effect.

Keywords: Cadmium porphyrin; X-ray molecular structure; UV/Vis spectroscopy; Fluorescence spectroscopy; Ligand effects.

Corresponding Author: E-mail: samir.acherar@univ-lorraine.fr. Phone: +33 037-274-3687**.**

Abbreviations: ATR for attenuated total reflectance; Cg for centroid; C_{im} for imidazole carbon atom; Ct for projection of the Cd(II metal ion in the porphyrinato mean plane; DMF for dimethylformamide; DMSO for dimethylsulfoxide; E_g for Gap energy; FTIR for Fourier transform infrared; L_{ax} for axial ligand; 2-MeHIm for 2-methylimidazole; MP for metalloporphyrin; N_{im} for imidazole nitrogen atom linked to the Cd(II) metal ion; NMR for nuclear magnetic resonance; N_p pyrrole nitrogen atom; TBPP (or H_2TBPP) for *meso*-tetrakis(4-tert-butylphenyl)porphyrin; TPP (or H_2TPP) for tetraphenylporphyrin; UV-Vis for ultraviolet-visible; ϕ for dihedral angle; ϕ_f for fluorescence quantum yield; τ_f for fluorescence lifetime.

1. Introduction

Porphyrins are a class of conjugated tetrapyrrole macrocycles consisting of four pyrrole units linked by four methine groups. The two pyrrole protons of the porphyrin free base can be easily removed and the resulting dianion species can complex a large variety of metal ions to form natural or synthetic metalloporphyrins (MPs). Among the various natural MPs and derivatives, some of them play a vital role in biological processes, such as oxygen transport (heme b), oxygen activation (cytochrome P450), photosynthesis (chlorophyll a), methanogenesis catalyst in methanogenic archaea (cofactor F430) or nervous system function (vitamin B12). Beyond their presence in nature, many synthetic MPs are chemically produced and used for catalytic oxidation reactions [1], biological applications [2] and material/device applications [3-8]. It is noteworthy that the spectroscopic, electrochemical, structural and photophysical properties of MPs are strongly dependent on the nature of the central metal ion and the axial coordination process can also deeply affect these properties [9]. Many of the group elements in the periodic table are able to form MPs and several among them are capable of coordinating to additional axial ligands. Among them, group 12 or II B (Zn, Cd, and Hg metals) occupies a special place because of the fact that it is the only group whose atoms or cations have a complete d sub-shell. Hg(II) and Cd(II) MPs are less studied due to their low stability compared to Zn(II) MPs. Despite the fact that Cd(II) is toxic metal ion, it has received much attention from researchers for over half a century because the Cd(II) metal ion is too large to fit into the central hole of porphyrins, thereby forming Cd(II) MPs with an out-of-plane metal coordination. This out-of-plane geometry greatly diminishes the stability of the Cd(II) porphyrin derivatives, making them good transmetallation precursors for metal-exchange reactions [10], and also is of particular interest for some biological applications [11-

13]. As the Cd(II) metal has just one oxidation state of +2, only one axial ligand can be coordinated to the Cd(II) metal ion to provide five-coordinate MPs (square pyramidal geometry) [14]. This geometry makes Cd(II)-porphyrins easy systems to study the influence of the nature of the axial ligand on the spectroscopic, electrochemical, structural and photophysical properties of MPs.

Imidazole and its derivatives are present in various biological compounds. For example, 2-methylimidazole (2-MeHIm) can be used to simulate the heme-coordinated histidine residue in biological hemoproteins [15] and is a precursor of several antibiotics of the nitroimidazole class to treat parasitic infections and anaerobic bacterial infections [16]. In the literature, we found several studies describing MPs (M = Fe(III), Fe(IV), Mn(II), Co(II), Co(III), Zn(II), Zr(IV) and Cr(III)) with one or two imidazole moieties as axial ligands [15-17]; to date no research has yet been carried out on the effect of an imidazole axial ligand upon the structural, spectroscopic and photophysical properties of Cd(II)-porphyrins.

In this work, we report the synthesis of a novel Cd(II)-porphyrin complex with one imidazole axial ligand, *i.e.* (2-methylimidazole)(*meso*-tetrakis(4-tert-butylphenyl)porphyrinato)cadmium(II), abbreviated as [Cd(TBPP)(2-MeHIm)] (**I**) (Scheme 1), with the aim to evaluate the influence of the *N*-donor axial ligand and out-of-plane geometry (square pyramidal) on the structural, spectroscopic and photophysical properties of the Cd(II)-porphyrin complex.

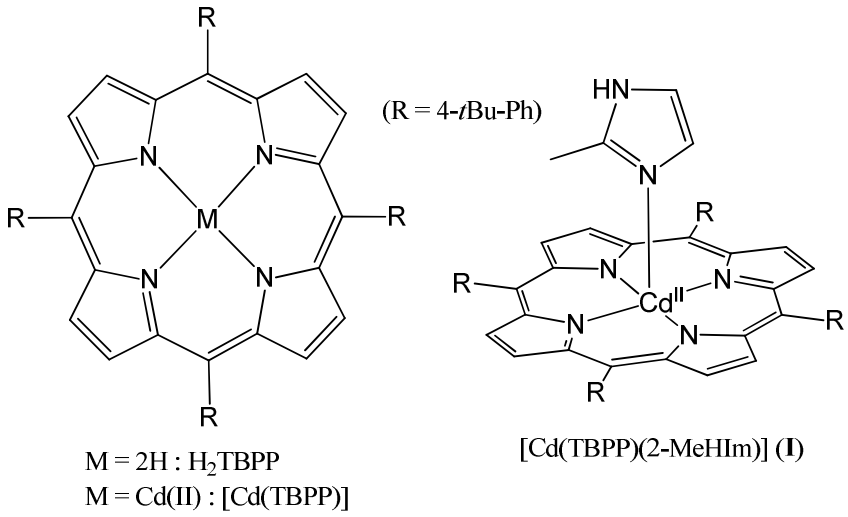

Scheme 1. Chemical structures of H_2TBPP, [Cd(TBPP)] and [Cd(TBPP)(2-MeHIm)].

2. Materials and methods

2.1. Chemicals

Unless otherwise stated, all chemicals were purchased as the highest purity commercially available and were used without further purification. Dry CH_2Cl_2 was obtained by distillation over P_2O_5 under an argon atmosphere and other reagent-grade solvents were used as received. The free base porphyrin H_2TBPP was purchased from the PorphyChem Company and $Cd(OAc)_2$ from Sigma-Aldrich.

2.2. Characterization

Infrared spectra were recorded with an attenuated total reflectance Fourier transform infrared (FTIR) Nexus (Nicolet) spectrophotometer with the wavenumber range 500-4000 cm^{-1}. ^1H NMR spectra were recorded on a Brucker Advance 300 spectrophotometer. The spectra were recorded in DMSO-*d6* at room temperature (T = 298 K) using DMSO residual peaks (δ = 2.50 ppm) as an internal reference. Chemical shifts (δ) are reported in parts per million (ppm). Coupling constants (*J*) are given in hertz (Hz) and the multiplicity is defined as s for singlet, d for doublet, m for multiplet, br for broad, *m*-Ph and *o*-Ph for *meta* and *ortho* protons of the phenyl rings, β-pyr for β protons on the pyrrole rings or combinations thereof. Element analyses were obtained with a Carlo Erba model 1106 microanalyzer (INEOS RAS).

2.3. UV-visible and fluorescence experiments

Ultraviolet-visible (UV-vis) absorption spectra were measured on a Shimadzu UV-3600 double-beam UV-visible spectrophotometer at a concentration of 10^{-5} M in CH_2Cl_2. Fluorescence spectra were recorded on a Fluorolog-3 spectrofluorometer FL3-222 at a concentration of 10^{-6} M in CH_2Cl_2. The fluorescence quantum yield (ϕ_f) was determined using a tetraphenyl porphyrin (TPP) solution in toluene as a fluorescence standard (ϕ_f = 0.11) [18].

2.4. X-ray crystallography experiment

Single crystals of the Cd(II)-porphyrin complex (**I**) were grown at room temperature from a $CHCl_3$-hexane mixture, carefully selected under a microscope and mounted on a Mitegen micromesh with the help of a trace of mineral oil. The X-ray diffraction experiment was

conducted using a Rigaku Oxford Diffraction Supernova diffractometer equipped with an Atlas CCD detector using MoKα radiation (λ = 0.7107 Å). Single crystals were cooled at 110 K by a low temperature nitrogen blower and diffraction frames were processed with the CrysAlisPRO program [19]. The first structure model solution was found with the SHELXS program [20] and model refinement was done with SHELXL2014/7 [21]. The CIF file was completed with Olex2 [22]. [Cd(TBPP)(2-MeHIm)] (**I**) was found to contain some disorders: (i) the 2-MeHIm axial ligand is disordered over two positions (N5-C61-C62-N6-C63-C64 and N5A-C61A-C3B1-N6A-C63A-C1AA) with occupancies values of 80 and 20%, respectively, (ii) four carbon atoms of one phenyl ring of the TBPP porhyrinate are disordered in two positions (C32-C33/C33A-C34A and C35-C36/C36A-C36A) with the same occupancy of 50/50%, (iii) the *t*-Bu group linked to this disordered phenyl ring, presents also two major positions (C37-C40 and C37A-C40A) with occupancy factor values of 0.65 and 0.35 respectively and (iv) a second *t*-Bu group of another phenyl group is equally disordered in two positions (50/50%).

The bond lengths and angles of the disordered fragments were restrained to ensure proper geometry using the DFIX and DANG instructions of SHELXL2014. The anisotropic displacement ellipsoids of some atoms of the porphyrin and the 2-methyimidazol axial ligand were very elongated, which indicates static disorder. For fragments involving these atoms DELU/SIMU and SIMU/ISOR restraints and the EADP constraint commands in SHELXL-2014 were used. At the final stages of the refinements of complex (**I**), we noticed the presence of two solvent voids in the cell of 446 $Å^3$ and 47 electrons for each one. Therefore, corrections for diffuse effects owing to the inclusion of two disordered hexane molecules in the crystal lattice of our TBPP-cadmium(II) porphyrin derivative (**I**) was made using the SQUEEZE subroutine in PLATON [23]. The given chemical formula of **(I)** and other crystal data of this complex do not take into account the two removed solvent molecules.

The crystallographic data, structural refinement details and selected bond lengths and angles for (**I**) are reported in Table SI-1 (see Supporting Information). Crystal data and experimental parameters used for the intensity data collection are available free of charge from the Cambridge Crystallographic Data Centre with CCDC number 1924229.

*2.5. Synthesis of the Cd(II)-porphyrin complex (**I**)*

[Cd(TBPP)] complex. The [Cd(TBPP)] complex was prepared by the insertion of the Cd(II) metal ion into the TBPP ring according to the protocol previously described in the literature

[24]. Briefly, to a solution of free porphyrin H_2TBPP (100 mg, 0.12 mmol) in DMF (15 mL) was added $Cd(OAc)_2$ (37 mg, 0.48 mmol). The reaction mixture was held at refluxing temperature (153 °C) with stirring for 15 min under a dry nitrogen atmosphere. The reaction mixture was reduced to dryness *in vacuo* and the residue was dissolved in benzene (10 mL); then *n*-hexane (100 mL) was added and the mixture was placed in a fridge (4 °C) overnight. [Cd(TBPP)] was isolated as a blue-black solid by filtration and vacuum-dried. Yield 108 mg (96%). Anal. Calcd for $C_{60}H_{60}CdN_4$ (%): C, 75.89; H, 6.37; N, 5.90. Found (%): C, 75.82; H, 6.24; N, 6.12. ^{1}H NMR (300 MHz, DMSO-d_6) δ, ppm: 1.61 (s, 36H, 4 *t*-Bu), 7.89 (d, 8H, *m*-Ph, J = 8.1 Hz), 8.05 (d, 8H, *o*-Ph, J = 8.1 Hz), 8.65 (s, 8H, *β*-pyr.). UV-vis (CH_2Cl_2) λ/nm (ε x 10^{-3}, mol^{-1} L cm^{-1}) : 433 (105), 569 (4), 613 (6). FTIR-ATR (CH_2Cl_2) wavenumber/cm^{-1}: 1038 ($\delta_{C\text{-}H}$, porphyrin), 2922 ($\nu_{C\text{-}H}$, porphyrin).

[Cd(TBPP)(2-MeHIm)] complex (**I**). The [Cd(TBPP)] complex (22 mg, 0.023 mmol) and 2-methylimidazole (47 mg, 0.57 mmol) were dissolved in $CHCl_3$ (8 mL) and the dark green reaction mixture was stirred overnight at room temperature. X-ray quality blue-purple crystals were obtained by liquid diffusion in a glass tube using hexane as the non-solvent. Yield 19 mg (80%). Anal. Calcd for $C_{69}H_{73}CdN_6$ (%): C, 75.42; H, 6.70; N, 7.64, Found (%): C, 75.48; H, 7.40; N, 7.81 ^{1}H NMR (300 MHz, DMSO-d_6) δ, ppm: 1.58 (s, 36H, 4 *t*-Bu), 2.41 (s, 3H, CH_3 imidazole), 6.86 (br s, 1H, H imidazole), 7.09 (br s, 1H, H imidazole), 7.83 (d, 8H, *m*-Ph, J = 8.1 Hz), 8.12 (d, 8H, *o*-Ph, J = 8.1 Hz), 8.72 (s, 8H, *β*-pyr.), 10.16 (br s, 1H, NH imidazole). UV-vis (CH_2Cl_2) λ/nm (ε x 10^{-3}, mol^{-1} L cm^{-1}): 438 (110), 579 (4), 621 (4). FTIR-ATR: wavenumber/cm^{-1}: 997 ($\delta_{C\text{-}H}$, porphyrin), 1456 ($\nu_{C\text{-}N}$, imidazole), 2854-2956 ($\nu_{C\text{-}H}$, porphyrin), 3433 ($\nu_{N\text{-}H}$, imidazole).

3. Results and discussion

3.1. Synthesis

The free base porphyrin H_2TBPP was metallated according to the literature procedure [24]. This metallation was carried out with an excess of $Cd(OAc)_2$ (4 equivalents) in DMF to afford the [Cd(TBPP)] complex in 96% yield (Scheme 2). The 14 nm red shift of the Soret band and the alteration in the number and position of Q bands in the UV-visible spectrum of [Cd(TBPP)], compared with that of H_2TBPP, confirmed that the metallation process occurred (see the section "UV-visible and fluorescence spectroscopies"). Further confirmation of the

metallation is given by the ^{1}H NMR spectral comparison of H_2TBPP and [Cd(TBPP)] in DMSO-d_6, showing the disappearance of the signal for the NH pyrrole protons at δ -2.74 ppm after metallation.

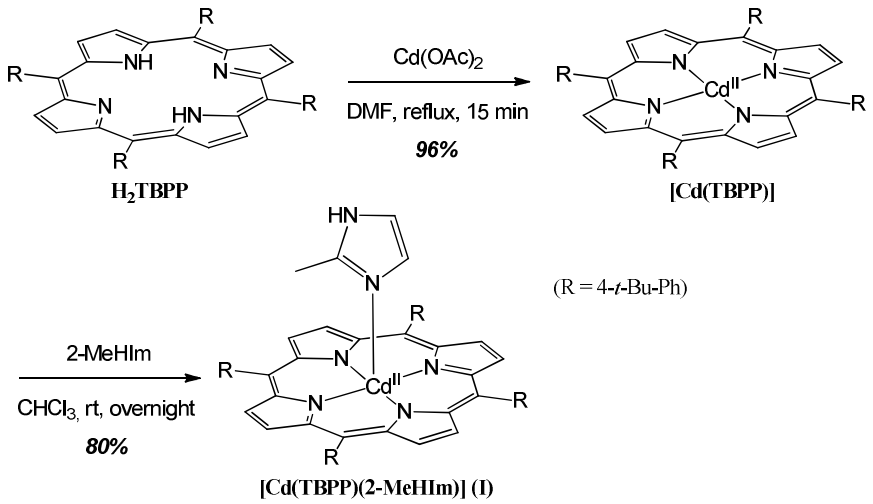

Scheme 2**.** Synthesis of the [Cd(TBPP)] and [Cd(TBPP)(2-MeHIm)] complexes.

The axial ligation of 2-methylimidazole (2-MeHIm) to the [Cd(TBPP)] complex was performed in $CHCl_3$, leading to the formation of [Cd(TBPP)(2-MeHIm)] complex (**I**) in 80% yield after recrystallization (Scheme 2). As axial ligation proceeded, a small red-shift of around 7-10 nm was observed for the Q bands of the [Cd(TBPP)(2-MeHIm)] complex compared with that of [Cd(TBPP)] (see the section "UV-visible and fluorescence spectroscopies"). Further confirmation of the 2-MeHIm *N*-donor axial ligand coordination is given by the ^{1}H NMR (DMSO-d_6) and IR absorption (CH_2Cl_2) spectra of complex (**I**). The ^{1}H NMR spectrum exhibits two sets of signals relating to the porphyrin moiety (δ = 1.58, 7.83, 8.12 and 8.72 ppm) and to the axial ligand (δ = 2.41, 6.86 and 7.09 ppm) (see Supporting Information, Figure SI-1a). In a similar way, the IR absorption spectrum simultaneously shows characteristic bands of the porphyrinato core (*i.e.*, C-H stretching bands at 2956-2854 cm^{-1} and C-H vibrational band at 997 cm^{-1}) and the axial ligand (*i.e.*, N-H and C-N stretching bands at 3433 and 1456 cm^{-1}, respectively) (see Supporting Information, Figure SI-1b).

3.2. X-ray crystal structure description

The title [Cd(TBPP)(2-MeHIm)] complex (**I**) crystallizes in the monoclinic system, space group $P2_1/c$, with lattice parameters a = 13.5105(5) Å, b = 41.2583(8) Å, c = 11.2226(4)Å, α

= γ = 90 °, β = 108.410(4)°, V = 5935.5(4) Å^3, Mr = 1031.62, ($C_{65}H_{66}CdN_6$), Z = 4. The single-crystal X-ray molecular structure of **I** is shown in Figure 1 and the main geometrical parameters are listed in Table 1.

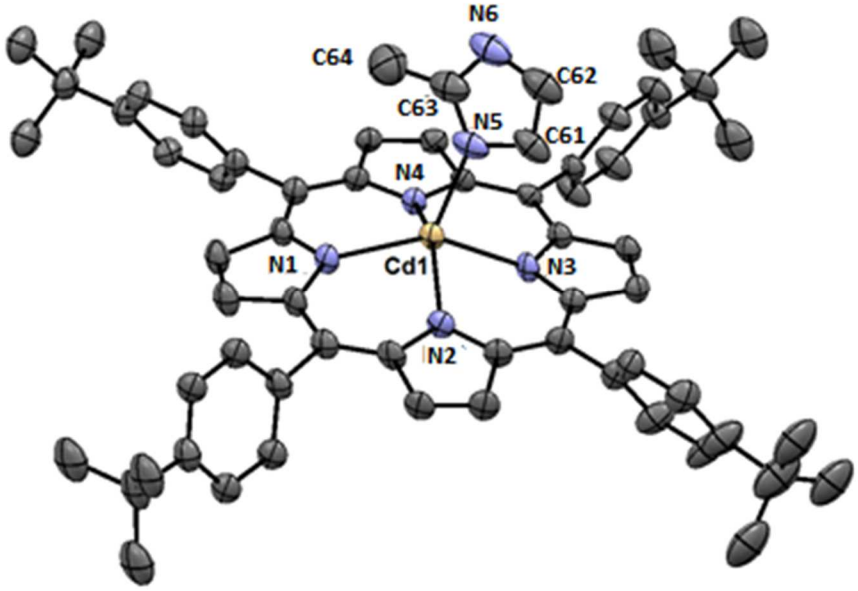

Figure 1. ORTEP view of the [Cd(TBPP)(2-MeHIm)] complex (**I**) showing the atom labelling, with 40% probability displacement ellipsoids. All H atoms are omitted for clarity and only the major positions of the disordered groups of **I** are shown.

Table 1. Selected bond lengths (Å) and dihedral angles (deg) of the [Cd(TBPP)(2-MeHIm)] complex (**I**).

Cadmium coordination polyhedron		
Bond lengths (Å)	**Dihedral angles (deg)**	
Cd-N1: 2.223(4)	N1-Cd-N2: 83.7(2)	N2-Cd-N4:143.2(2)
Cd-N2: 2.214(4)	N1-Cd-N3:141.9(2)	N2-Cd-N5: 111.8(2)
Cd-N3: 2.203(4)	N1-Cd-N4: 83.9(2)	N3-Cd-N4: 83.8(2)
Cd-N4: 2.215(4)	N1-Cd-N5: 94.3(2)	N3-Cd-N5: 123.6(2)
Cd-N5: 2.262(6)	N2-Cd-N3: 84.9(2)	N4-Cd-N5: 103.6(2)
Cd-N5A: 2.36(3)	N5A-Cd-N1: 104.4(9)	N5A-Cd-N3: 112.9(8)
	N5A-Cd-N2: 118(1)	N5A-Cd-N4: 98(1)
2-Methylimidazole (axial ligand)		
Bond lengths (Å)	**Dihedral angles (deg)**	
N5-C61: 1.37(1)	Cd-N5-C61: 124.3(5)	Cd-N5-C63: 131(2)
N5-C63: 1.379(5)	Cd-N5A-C63A: 116(2)	Cd-N5A-C61A: 123(2)
N5A-C61A: 1.378(5)		
N5A-C63A: 1.380(5)		

The asymmetric unit is made up of one isolated [Cd(TBPP)(2-MeHIm)] complex (**I**). The Cd(II) cation is chelated by the four pyrrole N atoms of the porphyrinate anion and additionally coordinated by the 2-MeHIm ligand in an apical site, completing the distorted square pyramidal coordination environment (Figure 2). The stereochemical parameters for **I** and other related five-coordinate Cd(II) porphyrin complexes are summarized in Table 2. For complex **I**, the displacement of the Cd(II) metal atom out of the porphyrinato mean plane (Cd•••C_t distance) is 0.860 Å and this value is slightly higher than in related five-coordinate Cd(II) porphyrin complexes reported in Table 2.

The value of the average equatorial distance between the cadmium cation and the four nitrogen atoms of the pyrrole rings (Cd–Np) is 2.214(4) Å, which is identical to that found in the $[Cd(TPP)(N_3)]^-$ ion complex, but slightly higher than the other related cadmium MPs (Table 2). In addition, the Cd-axial ligand distances (Cd-L_{ax}) are 2.36(3)/2.262(6) Å (for the two positions of the 2- MeHIm axial ligand), which are similar than those of the related five-coordinate Cd(II) porphyrin complexes (Table 2). The bond lengths and angles in the phenyl, pyrrole and imidazole rings are all in the normal range.

Table 2. Stereochemical parameters (Å)[a] of [Cd(TBPP)(2-MeHIm)] (**I**) and related five-coordinate cadmium porphyrin complexes.

Complex	**Cd-N_p** [b]	**Cd•••C_t** [c]	**Cd-L_{ax}** [d]	**Ref.**
[Cd(TBPP)(2-MeHIm)]	2.214(4)	0.860	2.36(3)/2.262(6)	this work
[Cd(TClPP)(py)]	2.203(4)	0.729	2.316(4)	[25]
[Cd(TClPP)(DMF)]	2.197	0.824	2.280	[25]
[Cd(TPP)(pip)]	2.204	0.751	2.323	[24]
[Cd(TPP)(4-picoline)]	2.195	0.744	2.298	[26]
[Cd(TPP)(2-NH_2-py)]	2.204(3)	0.739	2.316(3)	[27]
$[Cd(TPP)(N_3)]^-$	2.215(1)	0.796	2.238(2)	[28]

[a]: Estimated standard deviations are given in parentheses [b]: Cd-N_p is the average equatorial Cd-pyrrole nitrogen bond length, [c]: Cd•••C_t is the displacement of the Cd metal atom out of the porphyrinato mean plane, [d]: Cd-L_{ax} is the Cd-axial ligand bond length.

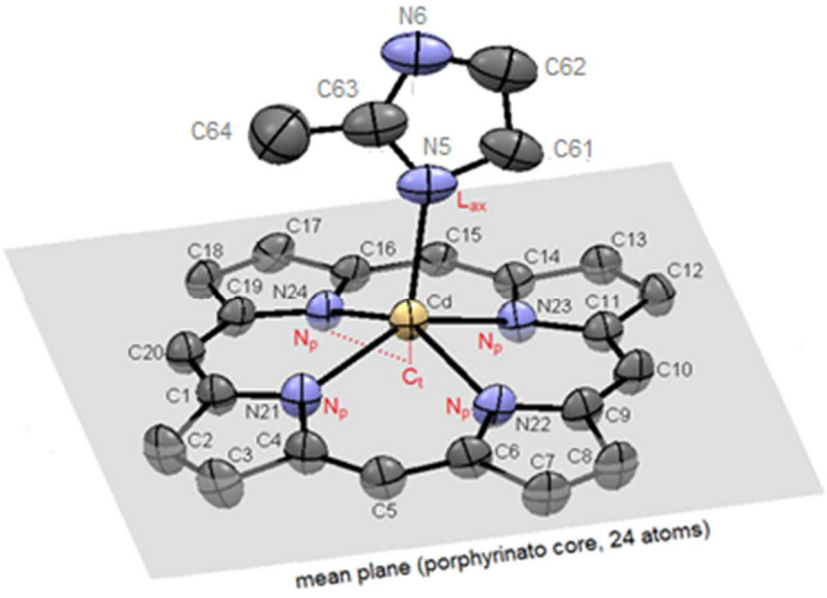

Figure 2**.** Distorted square pyramidal coordination geometry for complex **I**, showing the atom labelling. H atoms and *meso* groups are omitted for clarity and only the major position of the 2-MeHIm axial ligand is shown.

The values of the dihedral angles (ϕ) between the disordered 2-MeHIm planes, *i.e.* "N5-C63-N6-C62-C61" and "N5A-C63A-N6A-C62A-C61A", and the plane of the closest N_p-Cd-N_{im} plane, *i.e.* "N1-Cd-N5" and "N1-Cd-N5A" are 35.80/27.28°. These values are within the range of ϕ values observed for the related five-coordinate 2-MeHIm–MPs type [M^{II}(porphyrin)(2-MeHIm)] (M = Zn^{2+}, Fe^{2+}, Co^{2+} and Mn^{2+}) complexes (0° ≤ ϕ ≤ 44.5°, Table 3). We also noticed that the dihedral angles between Cd, N_{im} and the two imidazole carbon atoms (C_{im} atoms) linked to the N_{im} atoms are different. A larger dihedral angle of 131.38(6)/125.49(3) ° is found with the methyl group "C63"/ "C63A" carbon atom of the imidazole ligand ("Cd-N5-C63"/"Cd-N5A-C63A" dihedral angle, Table 3) compared with the values of 118.83°(7)/122.89.0°(4) for the "C61"/"C61A" carbon atom of the imidazole ligand ("Cd-N5-C61"/"Cd-N5A-C61A" dihedral angle, Table 3). This feature is also observed in the related five-coordinate [M^{II}(porphyrin)(2-MeHIm)] complexes and can be explained as being the result of the 2-MeHIm ring rotation which is needed to minimize the steric effect between this axial ligand and the porphyrinato core.

Table 3. Stereochemical parameters[a] of [Cd(TBPP)(2-MeHIm)] (**I**) and related five-coordinate [M^{II}(porphyrin)(2-MeHIm)] complexes (M = metal).

Complex	**M-N_p**[b,c]	**M•••C_t**[b,d]	**M-N_{im}**[b,e]	**M-N_{im}-C**[f,g]	**M-N_{im}-C**[f,h]	**ϕ** [f,i]	**Ref.**
Cd(II) metal ion							
[Cd(TBPP)(2-MeHIm)]	2.214(4)	0.860	2.36(3) 2.262(6)	131.38(6) 125.49(3)	118.83(7) 122.89(4)	35.80 27.28	this work
Zn(II) metal ion							
[Zn(Oetnp)(2-MeHIm)]	2.098(4)	0.46	2.106(4)	132.7(3)	120.4(3)	15.6	[29]
[Zn(Oetnp)(1-MeHIm)]	2.102(4)	0.46	2.122(4)	130.4(3)	122.7(3)	9.4	[29]
Fe(II) metal ion							
[Fe(TPP)(2-MeHIm)]	2.076(3)	0.39	2.144(1)	132.8(1)	121.4(1)	35.8	[30]
[Fe(TPP)(2-MeHIm)]	2.080(8)	0.41	2.120(2)	131.6(1)	122.4(1)	16.0	[30]
[Fe(TPP)(2-MeHIm)]	2.099(7)	0.55	2.099(2)	129.0(1)	125.7(1)	22.9	[31]
[Fe(TFPPBr_8)(2-MeHIm)]	2.077(3)	0.43	2.105(6)	130.5	123.8	0	[32]
[Fe(TMP)(2-MeHIm)]	2.07(1)	0.44	2.123(4)	127.1(4)	126.4(4)	19.3	[32]
[Fe(TMP)(2-MeHIm)]	2.08(2)	0.44	2.163(3)	132.1(3)	120.3(3)	9.6	[33]
[Fe(TTP)(2-MeHIm)]	2.076(3)	0.39	2.144(1)	132.8(1)	121.4(1)	35.8	[30]
[Fe(T*p*-OCH_3PP)(2-MeHIm)]	2.087(7)	0.51	2.155(2)	130.4(2)	123.4(2)	44.5	[30]
[Fe(OEP)(2-MeHIm)]	2.077(7)	0.46	2.135(3)	131.3(3)	122.4(3)	19.5	[32]
[Fe(TpivPP)(2-MeHIm)]	2.070(6)	0.38	2.113(3)	128.5(2)	125.7(3)	23.3	[17j]
Mn(II) metal ion							
[Mn(TpivPP)(2-MeHIm)]	2.129(3)	0.60	2.177(9)	126.4(7)	128.1(9)	28.1	[34]
Co(II) metal ion							
[Co(TpivPP)(2-MeHIm)]	1.979(3)	0.15	2.145(3)	132.0(3)	123.1(3)	21.6	[35]

[a]: Estimated standard deviations are given in parentheses. [b]: Value in angstroms. [c]: M-N_p is the average equatorial metal-pyrrole nitrogen bond length. [d]: M•••C_t is the displacement of the metal atom out of the porphyrinato mean plane. [e]: M-N_{Im} is metal-nitrogen axial ligand bond length. [f]: Value in degrees. [g]: Dihedral angle between the metal, the nitrogen atom of the axial ligand 2-MeHIm and the methyl substituted "C63"/"C63A" carbon atom of 2-MeHIm. [h]: Dihedral angle between the metal, the nitrogen atom of the axial ligand 2-MeHIm and the "C61"/"C61A" carbon atom of 2-MeHIm. [i]: Dihedral angle between the plane defined by the closest N_p-M-N_{im} and the imidazole plane.

As shown also in Table 3, the average equatorial metal-pyrrole nitrogen bond length (M-N_p), the metal-nitrogen axial ligand bond length (M-N_{Im}) and the displacement of the metal atom out of the porphyrinato mean plane (M•••C_t distance) in the related five-coordinate [M^{II}(porphyrin)(2-MeHIm)] complexes are consistent with the metal atomic radii. In fact, compared to other M metal ions (M = Fe^{2+}, Co^{2+} and Mn^{2+}), the Cd(II) cation has the largest atomic radius which implies that the Cd(II) metal ion is too large to fit into the central hole of

the porphyrin, thereby forming MP complexes with the largest out-of-plane displacements (M-N_p, M-N_{Im} and M•••C_t distances) based on the 24-atom mean plane. As a result, it can be seen that complex **I** exhibits higher values than the other related five-coordinate [M^{II}(porphyrin)(2-MeHIm)] complexes (M-N_p = 2.215(7) Å, M-N_{Im} =2.31(4)/2.278(6) Å and M•••C_t = 0.860 Å). These high values induce a significant porphyrinato core *doming* and a moderate *ruffling* indicated by the displacement of the *meso*-carbon atoms above and below the porphyrinato mean plane (see Supporting Information Figures SI-2 and SI-3) [30]. In accordance with the porphyrinato core *doming* for complex **I**, the displacement of 0.709 Å between the Cd(II) metal and the four pyrrole nitrogen atoms mean plane (*i.e.* N1-N2-N3-N4) is lower than that of the M•••C_t distance (0.860 Å).

The unit cell of the [Cd(TBPP)(2-MeHIm)] complex, shown in Figure 3, displays voids in the structure along the *b* and the *c* axes with an approximate volume of 781.15 $Å^3$ (~ 13.2% of the unit cell volume). On the other hand, the crystal lattice of [Cd(TBPP)(2-MeHIm)] exhibits intermolecular C-H···π interactions that stabilize the crystal packing *via* weak contacts involving the carbon atoms of the *t*-Bu group of the TBPP porphyrinato ligands and the centroids Cg2, Cg3 and Cg4 of the pyrrole rings and the imidazole centroid (Cg5) (Table 4, see Supporting Information Figure SI-4) of two adjacent [Cd(TBPP)(2-MeHIm)] molecules.

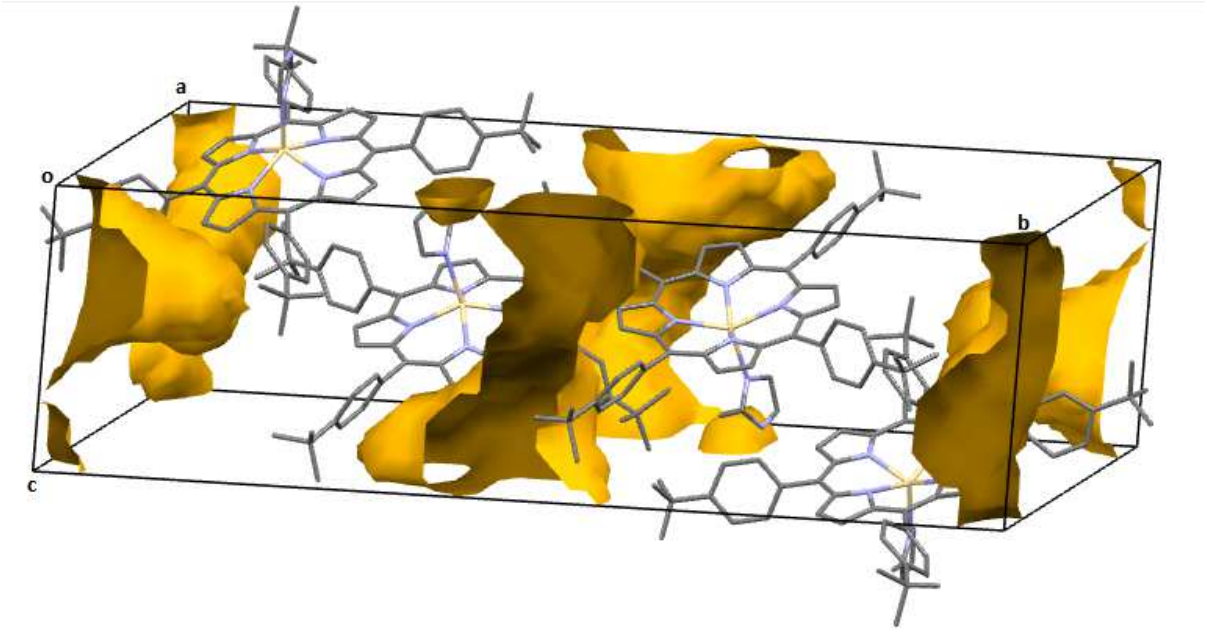

Figure 3. Packing diagram of the [Cd(TBPP)(2-MeHIm)] complex (**I**) showing voids in the *b* and *c* axes (in orange). The voids were calculated for a ball radius of 1.2 Å and a grid of 0.7 Å.

Table 4. Selected intermolecular C-H···π interactions for the [Cd(TBPP)(2-MeHIm)] complex (**I**).

D-H···A [a]	**Symmetry of A**	**D-H···A (Å)**	**D-H···A (deg)**
C30-H30B···Cg3[b]	-1+x,y,z	3.455(2)	116
C52-H52···Cg4[c]	x,3/2-y,1/2+z	3.395(7)	137
C18-H18···Cg5[d]	x,3/2-y,-1/2+z	3.714(7)	133
C38-H38···Cg5[e]	1-x,1-y,-1-z	3.58(1)	157

[a]: D is the donor atom and A is the acceptor atom, [b]: Cg3 is a pyrrole centroid (*i.e.* C11-C12-C13-C14-N3), [c]: Cg4 is a pyrrole centroid (*i.e.* C16-C17-C18-C19-N4) and [e]: Cg5 is the imidazole centroid (*i.e.* N5A-C61A-C62A-N6A-C63A).

3.3. UV-visible and fluorescence spectroscopies

The UV-visible spectra of MPs exhibit two types of absorption bands: one strong band, known as the Soret band (or B band) at around 400 nm, and two weak Q bands (Q(1,0) and Q(0,0)) located between 500 and 700 nm. The UV-visible absorption spectra in CH_2Cl_2 (c = 10^{-5} M) of the free base porphyrin (H_2TBPP), the starting material ([Cd(TBPP)]) and the cadmium MP complex **I** ([Cd(TBPP)(2-MeHIm)]) are illustrated in Figure 4a. The λ_{max} values of the Soret and Q bands for [Cd(TBPP)] (433, 569 and 613 nm) and the [Cd(TBPP)(2-MeHIm)] complex (**I**) (438, 579 and 621 nm) indicate a red-shift of these bands compared to the free base H_2TBPP (Figure 4a and Table 5). As shown in Table 5, the insertion of the Cd(II) metal ion into the TBPP ring induces an higher red-shift of the absorption bands compared to other metal(II) ions (M = Zn, Cu, Ni, Co) and this red-shift phenomenon increases with the complexation of the 2-MeHIm axial ligand. The red-shift displacement of the spectrum for our Cd(II) complex **I** is also higher than that found in related five-coordinate Cd(II) porphyrin complexes (Table 5). The higher red-shift of the absorption bands in **I** can be explained by the significant *doming* distortion of the TBPP macrocycle [36]. The higher atomic radius of the Cd(II) metal ion compared to the other metals (M = Zn, Cu, Ni, Co) (Table 5) implies that the Cd(II) ion is too large to fit into the central hole of the TBPP, which generates significant deformation of the TBPP porphyrin core and the complexation of the 2-MeHIm *N*-donor axial ligand tends to increase the *doming* distortion by pulling the Cd(II) metal ion out of the porphyrinato plane.

The optical band gap energy (E_g) refers to the energy difference between HOMO and LUMO levels. The E_g value is an important measurement in semiconductor and nanomaterial industries and can be estimated from an UV-visible spectrum. The E_g values for H_2TBPP,

[Cd(TBPP)] and [Cd(TBPP)(2-MeHIm)] (**I**) were calculated using Tauc plots [37] and following the equation based on the Plank's quantum theory:

$$E_g\ (eV) = \frac{h \times c}{\lambda_{gap}} = \frac{1240}{\lambda_{gap}}$$

where *h* is Plank's constant, *c* is the velocity of light and λ_{gap} (in nm) is the wavelength value of the tangent to the Q(0,0) absorption band.

The E_g values in CH_2Cl_2 solution are estimated to be around 1.95 and 1.92 eV for the complexes [Cd(TBPP)] and **I**, respectively, which are higher than that of the H_2TBPP free base (1.85 eV) suggesting that the materials display interesting organic semiconducting properties [38].

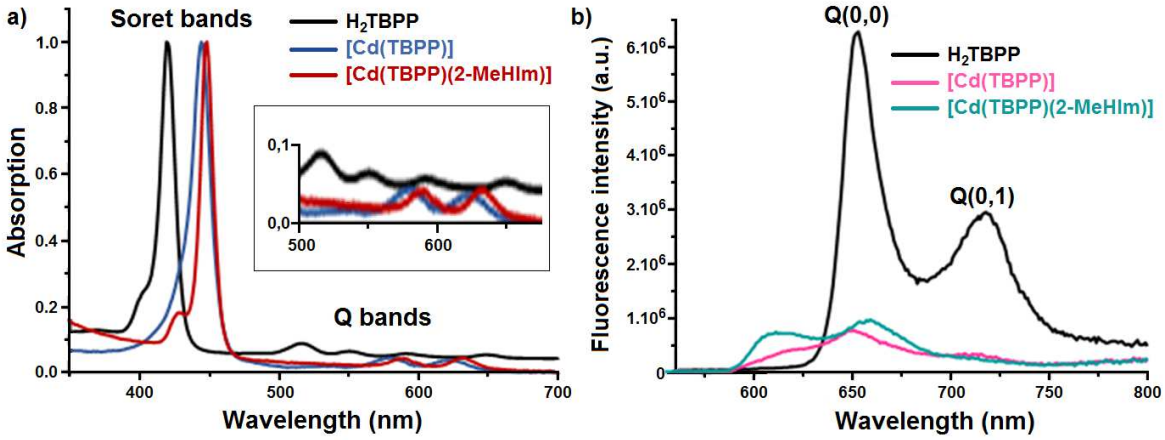

Figure 4. (a): UV-visible absorption spectra in CH_2Cl_2 (c = 10^{-5} M) and (b): fluorescence emission spectra in CH_2Cl_2 (c = 10^{-6} M) of H_2TBPP, [Cd(TBPP)] and [Cd(TBPP)(2-MeHIm)] (**I**) (λ_{exc} = 433 nm).

Table 5. UV-visible data of H_2TBPP, [Cd(TBPP)], [Cd(TBPP)(2-MeHIm)] (**I**) and related metalloporphyrins.

Compound	**Soret Band** (nm, logε)	**Q bands** (nm, logε)	**Ref.**
H_2TBPP and related [M^{II}(TBPP)] complexes			
H_2TBPP[a]	419 (4.6)	519 (5.60), 557 (3.04), 589 (2.9), 650 (2.6)	this work
[Cd(TBPP)][a]	433 (4.02)	569 (2.8), 613 (2.6)	this work
[Zn(TBPP)][a]	420	550, 570	[39]
[Cu(TBPP)][b]	419	543, 609	[40]
[Mg(TBPP)][b]	431	565, 610	[40]
[Ni(TBPP)][b]	418	531, 619	[41]

[Co(TBPP)][b]	412	529, -	[42]
Five-coordinate [Cd^{II}(porphyrin)(ligand)] complexes			
[Cd(TBPP)(2-MeHIm)][b]	438 (4.04)	579 (2.65), 621 (2.60)	this work
[Cd(TPP)(2-NH_2-py)][d]	429 (3.01)	—	[27]
[Cd(TClPP)(py)][b]	433 (4.49)	567 (3.20), 609 (3.14)	[25]
[Cd(TClPP)(DMF)][b]	433 (4.49)	567 (3.20), 609 (3.14)	[25]

[a]: in CH_2Cl_2. [b]: in N-méthyl-2-pyrrolidone. [c]: in acetone.

The fluorescence emission spectra of the free base porphyrin (H_2TBPP), [Cd(TBPP)] and [Cd(TBPP)(2-MeHIm)] (**I**) at room temperature were recorded in CH_2Cl_2 ($c = 10^{-6}$ M) under an excitation wavelength of 433 nm (Figure 4b). Table 6 summarizes the maxima of the fluorescence of the Q(0,0) and Q(0,1) bands, the fluorescence quantum yields (ϕ_f) and the fluorescence lifetimes (τ_f) of our derivative and other related free base porphyrins, MPs and five-coordinate MP complexes. The emission spectrum of the free base porphyrin (H_2TBPP) in CH_2Cl_2 displays two emission Q bands at 650 and 717 nm (Q(0,0) and Q(0,1), respectively), similar to those obtained for *meso*-tetrakis(phenyl)porphyrin (H_2TPP) and *meso*-tetrakis(4-tolyl))porphyrin (H_2TTP) in CH_2Cl_2 (Table 6). Compared to the free base porphyrin H_2TBPP, the emission spectrum of [Cd(TBPP)] shows a 36 nm (from 650 to 614 nm) and a 67 nm (from 717 to 650 nm) blue-shift for the Q(0,0) and Q(0,1) bands, respectively, followed by a decrease of the fluorescence emission, ϕ_f and τ_f (Figure 4b). Thus, metallation of H_2TBPP results in a remarkable hypsochromic effect in the fluorescence spectrum (Table 6), indicating that the structure of the originally planar porphyrin (free base porphyrin H_2TBPP) is out-of-plane distorted in [Cd(TBPP)] and the decrease of the ϕ_f value is the consequence of the distortion, which promotes other non-radiative energy dissipation processes than light emission. Other out-of-plane tetracoordinated MPs, like [Cd(TPP)], [Zn(TPP)], [Zn(TTP)] and [Mg(TPP)], have shown similar emission tendencies of the band-shift and quantum yield (Table 6). The fluorescence emission spectrum of [Cd(TBPP)(2-MeHIm)] (**I**) is quite similar to that of [Cd(TBPP)] and shows that the coordination of the 2-MeHIm *N*-donor axial ligand to the Cd(II) metal ion has a minor effect on the photophysical properties. This result suggests that the out-of-plane distortions of the porphyrin rings in the [Cd(TBPP)] and [Cd(TBPP)(2-MeHIm)] (**I**) complexes are relatively similar and consistent with the literature data, which state that the coordination of an axial ligand to a MP does not affect the fluorescence emission spectra (*e.g.* comparison between [Zn(TPP)] and [Zn(TPP)(Ligand)] complexes and between [Mg(TPP)] and [Mg(TPP)(2-N_3)$^-$] complexes) (Table 6). In addition, we noted that the ϕ_f values of the [Cd(TBPP)] and [Cd(TBPP)(2-

MeHIm)] complexes are also lower than those of the Zn(II) and especially Mg(II) complexes. This is also explained by the high molar mass of the Cd(II) ion, which leads to a quenching effect, resulting in the very low ϕ_f values [43].

Table 6. Fluorescence emission data of H_2TBPP, [Cd(TBPP)], [Cd(TBPP)(2-MeHIm)] (**I**), [M^{II}(porphyrin)] and [M^{II}(porphyrin)(ligand)] complexes (M = Cd, Zn and Mg).

Compound	**Q(0,0) (nm)**	**Q(0,1) (nm)**	ϕ_f	τ_f **(ns)**	**Solvent (concentration)**	λ_{exc} **(nm)**	**Ref.**
Free base porphyrins							
H_2TPP	656	717	0.09	—	CH_2Cl_2 (2.10^{-5} M)	—	[44]
H_2TTP	655	717	0.09	8.6	CH_2Cl_2 (2.10^{-5} M)	—	[44]
H_2TBPP	650	717	0.08	8.9	CH_2Cl_2 (10^{-6} M)	433	this work
[Cd^{II}(porphyrin)] and [Cd^{II}(porphyrin)(ligand] complexes							
[Cd(TPP)]	—	—	0.0004	0.065	methylcyclohexane (—)	—	[45]
[Cd(TBPP)]	614	650	0.01	1.6	CH_2Cl_2 (10^{-6} M)	433	this work
[Cd(TBPP)(2-MeHIm)]	612	657	0.02	1.7	CH_2Cl_2 (10^{-6} M)	433	this work
[Zn^{II}(porphyrin)] and [Zn^{II}(porphyrin)(ligand] complexes							
[Zn(TPP)]	597	647	0.037	1.9 [a]	CH_2Cl_2 (2.10^{-5} M)	600	[44,46]
[Zn(TTP)]	600	648	0.031	1.6	CH_2Cl_2 (2.10^{-5} M)	590	[44]
$[Zn(TPP)(N_3)]^-$	594	643	0.036	1.7	CH_2Cl_2 (10^{-6} M)	560	[47]
$[Zn(TPP)(NCO)]^-$	594	642	0.047	1.7	CH_2Cl_2 (10^{-6} M)	560	[47]
$[Zn(TPP)(NCS)]^-$	593	643	0.028	1.7	CH_2Cl_2 (10^{-6} M)	560	[47]
$[Zn(TPP)(CN)]^-$	594	643	0.055	1.7	CH_2Cl_2 (10^{-6} M)	560	[47]
[Mg^{II}(porphyrin)] and [Mg^{II}(porphyrin)(ligand] complexes							
[Mg(TPP)]	608	665	0.15 [b]	9.2 [b]	CH_2Cl_2 (—)	550	[45,48]
$[Mg(TPP)(N_3)]^-$	609	663	0.10	3.7	CH_2Cl_2 (10^{-6} M)	560	[49]
$[Mg(TPP)(NCO)]^-$	609	664	0.18	3.8	CH_2Cl_2 (10^{-6} M)	560	[49]
$[Mg(TPP)(NCS)]^-$	608	662	0.19	6.1	CH_2Cl_2 (10^{-6} M)	560	[49]

[a]: In MeTHF solvent. [b]: In methylcyclohexane solvent.

4. Conclusion

In this work, we described the Cd(II) metallation of the *meso*-tetrakis(4-tert-butylphenyl)porphyrinato (TBPP), followed by the 2-MeHIm *N*-donor axial ligand coordination. The structure of the [Cd(TBPP)(2-MeHIm)] complex (**I**) was determined by a single-crystal X-ray diffraction experiment, which revealed that Cd(II) metal ion induces a significantly distorted five-coordinate square pyramidal geometry. The displacement of the

Cd(II) metal atom out of the porphyrinato mean plane is 0.860 Å and this value is slightly higher than in related [Cd(II)(porphyrin)(ligand)] complexes. This high value induces a significant porphyrinato core *doming* and a moderate *ruffling*. H_2TBPP, [Cd(TBPP)] and [Cd(TBPP)(2-MeHIm)] (**I**) were characterized by ^{1}H NMR, FTIR, UV-visible and fluorescence spectroscopies. The UV-visible spectra showed that the insertion of the Cd(II) metal ion into the TBPP ring induces a red-shift of the absorption bands and this phenomenon is greater when the 2-MeHIm axial ligand is coordinated. The calculation of the gap energy (E_g) suggested that the [Cd(TBPP)] and [Cd(TBPP)(2-MeHIm)] (**I**) complexes display interesting organic semiconducting properties. The fluorescence emission spectra showed a remarkable blue-shift effect in the Q bands, accompanied by a decrease of fluorescence emission, quantum yield (ϕ_f) and lifetime (τ_f) after the insertion of the Cd(II) metal ion into the TBPP ring and the coordination of the 2-MeHIm axial ligand has a minor effect. These results indicate that the structure of the originally planar porphyrin (free base porphyrin H_2TBPP) is distorted in the out-of-plane MP ([Cd^{II}(TBPP)]) and the decrease in ϕ_f is the consequence of mainly the high quenching effect of the heavy cadmium metal and also the distortion of the porphyrin core, which promotes the loss of the "motion energy" by other non-radiative energy dissipation processes than light emission.

Acknowledgments

The authors acknowledge Mr. O. Fabre for running the NMR experiments, Dr. E. Wenger for performing XRD experiments and Dr. P. Arnoux for performing spectroscopic experiments.

Appendix B. X-ray crystallography data

CCDC 1924229 contains the supplementary crystallographic data for complex **I**. These data can be obtained free of charge via http://www.ccdc.cam.ac.uk/conts/retrieving.html, or from the Cambridge Crystallographic Data Centre, 12 Union Road, Cambridge CB2 1EZ, UK; fax: (+44) 1223-336-033; or e-mail: deposit@ccdc.cam.ac.uk.

References

[1] J. C. Barona-Castaño, C. C. Carmona-Vargas, T. J. Brocksom, K. T. de Oliveira, Molecules, 21 (2016) 310.

[2] a) R. Chandra, M. Tiwari, P. Kaur, M. Sharma, R. Jain, S. Dass, Indian J. Clin. Biochem., 15 (2000) 83–99; b) H. Huang, W. Song, J. Rieffel, J. F. Lovell, Front. Phys., 3 (2015) 1–15; c) M. Imran, M. Ramzan, A. K. Qureshi, M. A. Khan, M. Tariq, Molecules, 8 (2018) 95.

[3] M. K. Nazeeruddin, R. Humphry-Baker, D. L. Officer, W. M. Campbell, A. K. Burrell, M. Grätzel, Langmuir, 20 (2004) 6514–6517.

[4] a) H. L. Anderson, S. J. Martin, D. D. C. Bradley, Angew. Chem. Int. Ed. Engl., 33 (1994) 655–657; b) T. E. Screen, J. R. Thorne, R. G. Denning, D. G. Bucknall, H. L. Anderson, J. Am. Chem. Soc., 124 (2002) 9712–9713.

[5] a) M. J. Crossley, P. L. Burn, J. Chem. Soc., Chem. Commun., (1991) 1569–1571; b) T. Ishida, Y. Morisaki, Y. Chujo, Tetrahedron Lett., 47 (2006) 5265–5268.

[6] a) D. Wróbel, J. Łukasiewicz, J. Goc, A. Waszkowiak, R. Ion, J. Mol. Structure, 555 (2000) 407–416; b) K. Takechi, T. Shiga, T. Motohiro, T. Akiyama, S. Yamada, H. Nakayama, K. Kohama, Sol. Energy Mater. Sol. Cells, 90 (2006) 1322–1330.

[7] Y. Li, L. Cao, H. Tian, J. Org. Chem., 71 (2006) 8279–8782.

[8] L. Lvova, C. Di Natale, R. Paolesse, Sens. Actuator B-Chem, 179 (2012) 21–31.

[9] I. Bouamaied, T. Coskun, E. Stulz in Non-Covalent Multi-Porphyrin Assemblies. Structure and Bonding, (Ed.E. Alessio), Springer, Berlin, Heidelberg, Vol. 121 (2006) 1–47.

[10] a) A. Shamim, P. Hambright, J. Inorg. Nucl. Chem., 42 (1980) 1645–1647; b) R. A. Vilaplana, F. González-Vilchez, J. Chem. Soc., Dalton Trans., (1993) 1779–1781; c) A. Robert, B. Meunier, Chem. Eur. J., 4 (1998) 1287–1296; c) S. V. Zvezdina, O. M. Kulikova, N. Zh. Mamardashvili, Russ. J. Gen. Chem., 83 (2013) 2103–2017.

[11] E. Nyarko, M. Tabata, J. Porphyr. Phthalocyanines, 5 (2001) 873–880.

[12] M. Tabata, A. Kumar Sarker, E. Nyarko, J. Inorg. Biochem., 94 (2003) 50–58.

[13] E. Nyarko, T. Hara, D. J. Grab, M. Tabata, T. Fukuma, Chem. Biol. Interact., 139 (2002) 177–185.

[14] C. O. Chin, Inorg. Chem. Acta, 187 (1991) 221–225.

[15] F. Gruia, X. Ye, D. Ionascu, M. Kubo, P. M. Champion, Biophys. J., 93 (2007) 4404–4413.

[16] a) D. I. Edwards, J. Antimicrob. Chemother., 31 (1993) 9–20; b) K. Ebel, H. Koehler, A. O. Gamer, R. Jäckh, in Ullmann's Encyclopedia of Industrial Chemistry, Wiley-VCH Verlag GmbH & Co. KGaA, Weinheim, Vol. 18 (2000) 637–645.

[17] a) P. E. Ellis JR, R. D. Jones, F. Basolo, Proc. Natl. Acad. Sci. USA, 76 (1979) 5418–5420; b) W. R. Scheidt, D. K. Geiger, Y. Ja Lee, C. A. Reed, G. Lang, J. Am. Chem. Soc., 107 (1985) 5693–5699; c) G. Levey, D. A. Sweigart, J. G. Jones, A. L. Prignano, J. Chem. Soc., Dalton Trans., (1992) 605–607; d) M. Inamo, K. Nakajima, Bull. Chem. Soc. Jpn., 71 (1998) 883–891; e) S. De Lauzon, D. Mansuy, J.-P. Mahy, Eur. J. Biochem., 269 (2002) 470–480; f) A. Takahashi, T. Kurahashi, H. Fujii, Inorg. Chem., 48 (2009) 2614–2625; g) R. Patra, A. Chaudhary, S. K. Ghosh, S. P. Rath, Inorg. Chem., 49 (2010) 2057–2067; h) E. V. Motorina, T. N. Lomova, Russ. J. Gen. Chem., 80 (2010) 842–848; i) E. Mishra, J. L. Worlinsky, T. M. Gilbert, C. Brückner, V. Ryzhov, J. Am. Soc. Mass Spectrom., 23 (2012) 1135–1146; j) J. Li, B. C. Noll, A. G. Oliver, C. E. Schulz, W. R. Scheidt, J. Am. Chem. Soc., 135 (2013) 15627–15641; k) X. Y. Liu, X. N. Zhang, N. X. Li, Int. J. Environ. Res., 9 (2015) 961–968; l) Y. Tan, N. Escorcia, A. Hyslop, E. Wang, Anal. Chem. Res., 3 (2015) 70–76; m) S.-J. Wang, Y.-L. Peng, C.-G. Zhang, Y.-B. Li, C. Liu, Bull. Korean Chem. Soc., 36 (2015) 2693–2702; n) J. A. Serth-Guzzo, I. Turowska-Tyrk, M. K. Safo, F. A. Walker, P. G. Debrunner, W. R. Scheidt, J. Porphyr. Phthalocyanines, 20 (2016) 254–264; o) W. Sun, J. Li, Acta Cryst., E72 (2016) 1116–1120.

[18] P. G. Seybold, M. Gouterman, J. Mol. Spectrosc., 31 (1969) 1–13.

[19] CrysAlis PRO, Agilent (2014), Agilent Technologies Ltd, Yarnton, Oxfordshire, England.

[20] G. M. Sheldrick, Acta Cryst., A71 (2015) 3–8.

[21] P. W. Betteridge, J. R. Carruthers, R. I. Cooper, K. Prout, D. J. Watkin, J. Appl. Cryst., 36 (2003) 1487.

[22] O. V. Dolomanov, L. J. Bourhis, R. J. Gildea, J. A. K. Howard, H. Puschmann, J. Appl. Cryst., 42 (2009) 339–341.

[23] S. AL. Acta Crystallog. Sect. D65 (2009) 148–155.

[24] P. F. Rodesiler, E. A. H. Griffith, N. G. Charles, L. Lebioda, E. L. Amma, Inorg. Chem., 24 (1985) 4595–4600.

[25] W.-S. Wun, J.-H. Chen, S.-S. Wang, J.-Y. Tung, F.-L. Liao, S.-L. Wang, L.-P. Hwang, S. Elango, Inorg. Chem. Commun., 7 (2004) 1233–1237.

[26] M. P. Byrn, C. J. Curtis, I. Goldberg, Y. Hsiou, S. I. Khan, P. A. Sawin, S. K. Tendick, C. E. Strouse, J. Am. Chem. Soc., 113 (1991) 6549–6557.

[27] P. S. Zhao, F. F. Jian, L. Zhang, Bull. Korean Chem. Soc., 27 (2006) 1053–1055.

[28] H. Toumi, N. Amiri, M. S. Belkhiria, J.-C. Daran, H. Nasri, Acta Crystallogr. Sect. E Struct. Rep. Online, 68 (2012) m1557–m1158.

[29] M. O. Senge, J. Porphyr. Phthalocyanines, 2 (1998) 107–121.

[30] C. Hu, A. Roth, M. K. Ellison, J. An, C. M. Ellis, C. E. Schulz, W. R. Scheidt, J. Am. Chem. Soc., 127 (2005) 5675–5688.

[31] C. Hu, B. C. Noll, P. M. B. Piccoli, A. J. Schultz, C. E. Schulz, W. R. Scheidt, J. Am. Chem. Soc., 130 (2008) 3127–3136.

[32] B. Hu, M. He, Z. Yao, C. E. Schulz, J. Li, Inorg. Chem., 55 (2016) 9632–9643.

[33] C. Hu, B. C. Noll, C. E. Schulz, W. R. Scheidt, Inorg. Chem., 44 (2005) 4346–4358.

[34] Q. Yu, Y. Liu, D. Liu, J. Li, Dalton Trans., 44 (2015) 9382–9390.

[35] J. Li, B. C. Noll, A. G. Oliver, G. Ferraudi, A. G. Lappin, W. R. Scheidt, Inorg. Chem., 49 (2010) 2398–2406.

[36] a) Z. Valicsek, O. Horváth, G. Lendvay, I.Kikaš, I. Škorić, J. Photochem. Photobiol. A: Chem., 218 (2011) 143–155; b) Z. Valicsek, O. Horváth, Microchem. J., 107 (2013) 47–62.

[37] J. Tauc, R. Grigorovici, A. Vancu, Phys. Status Solidi B, 15 (1966) 627–637.

[38] F. Mulya, G. A. Santoso, H. A. Aziz, H. D. Pranowo, AIP Conf. Proc., 1755 (2016) 1–5.

[39] D. K. Panda, F. S. Goodson, S. Ray, R. Lowell, S. Saha, Chem. Commun., 48 (2012) 8775–8777.

[40] M. O. Liu, C-H. Tai, A. T. Hu, Mater. Chem. Phys., 92 (2005) 322–326.

[41] S. Richeter, A. Hadj-Aïssa, C. Taffin, A. Van Der Lee, D. Leclercq, Chem. Commun., (2007) 2148–2150.

[42] E. Jaworska, M. L. Naitana, E. Stelmach, G. Pomarico, M. Wojciechowski, E. Bulska, K. Maksymiuk, R. Paolesse, A. Michalska, Anal. Chem., 89 (2017) 7107–7114.

[43] U. Tripathy, D. Kowalska, X. Liu, S. Velate, R. P. Steer, J. Phys. Chem. A, 112 (2008) 5824–5833.

[44] E. J. Shin, D. Kim, Photochem. Photobiol. A: Chem., 152 (2002) 25–31.

[45] A. Harriman, J. Chem. Soc., Faraday Trans. 2, 77 (1981) 1281–1291.

[46] S. Gentemann, C. J. Medforth, T. P. Forsyth, D. J. Nurco, K. M. Smith, J. Fajer, D. Holten, J. Am. Chem. Soc., 116 (1994) 7363–7368.

[47] Z. Denden, K. Ezzayani, E. Saint-Aman, F. Loiseau, S. Najmudin, C. Bonifácio, J.-C. Daran, H. Nasri, Eur. J. Inorg. Chem., (2015) 2596–2610.

[48] J. Zhang, P. Zhang, Z. Zhang, X. Wei, J. Phys. Chem. A, 113 (2009) 5367–5374.

[49] K. Ezzayani, Z. Denden, S. Najmudin, C. Bonifácio, E. Saint-Aman, F. Loiseau, H. Nasri, Eur. J. Inorg. Chem., (2014) 5348–5361.

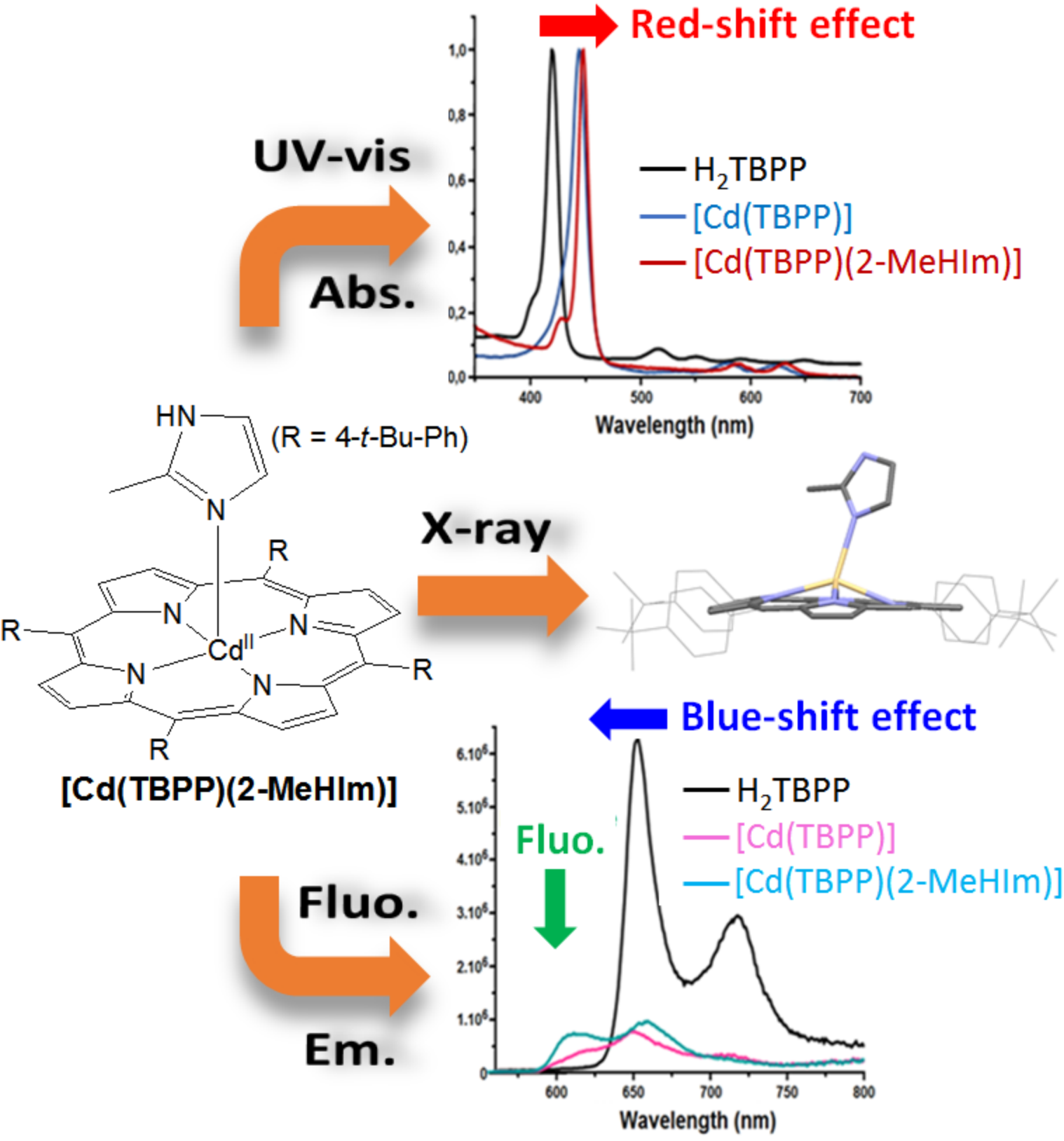
Red-shift effect
UV-vis
Abs.
H2TBPP
[Cd(TBPP)]
[Cd(TBPP)(2-MeHIm)]
Wavelength (nm)
HN
(R = 4-t-Bu-Ph)
N
R
N
N
Cd II
N
N
R
R
R
[Cd(TBPP)(2-MeHIm)]
X-ray
Blue-shift effect
Fluo.
H2TBPP
[Cd(TBPP)]
[Cd(TBPP)(2-MeHIm)]
Fluo.
Em.
Wavelength (nm)